Photothermal determination of thermal diffusivity and polymerization depth profiles of polymerized dental resins

P. Martínez-Torres,[1,a)] A. Mandelis,[2] and J. J. Alvarado-Gil[1]
[1]*Department of Applied Physics, CINVESTAV-Unidad Mérida, Antigua Carretera a Progreso Km. 6, 97310 Mérida, Mexico*
[2]*Department of Mechanical and Industrial Engineering, Center for Advanced Diffusion-Wave Technologies (CADIFT), University of Toronto, 5 King's College Road, Toronto, Ontario M5S 3G8, Canada*

(Received 2 October 2009; accepted 26 October 2009; published online 3 December 2009)

The degree and depth of curing due to photopolymerization in a commercial dental resin have been studied using photothermal radiometry. The sample consisted of a thick layer of resin on which a thin metallic gold layer was deposited, thus guaranteeing full opacity. Purely thermal-wave inverse problem techniques without the interference of optical profiles were used. Thermal depth profiles were obtained by heating the gold coating with a modulated laser beam and by performing a frequency scan. Prior to each frequency scan, photopolymerization was induced using a high power blue light emitted diode (LED). Due to the highly light dispersive nature of dental resins, the polymerization process depends strongly on optical absorption of the blue light, thereby inducing a depth dependent thermal diffusivity profile in the sample. A robust depth profilometric method for reconstructing the thermal diffusivity depth dependence on degree and depth of polymerization has been developed. The thermal diffusivity depth profile was linked to the polymerization kinetics.
 [doi:10.1063/1.3266007]

I. INTRODUCTION

For several years photothermal techniques have been applied successfully to the nondestructive study of materials.[1–3] Progress in the photothermal sciences has been made mainly due to continued improvements in the development of light sources, transducers, and equipment for data collection and processing.[1,2,4,5] In particular, photothermal radiometry (PTR) is one of the most important techniques because this detection method involves nondestructive, noncontact remote sensing. The technique consists of directing a modulated light beam onto the sample. The resulting periodic heat flux into the sample produces a periodic temperature distribution, which is called "thermal wave." As a result, infrared (IR) Planck radiation is emitted and subsequently detected by an IR detector. The thermal diffusion length is governed by the thermal diffusivity and the modulation frequency. Since the thermal diffusivity depends, among other things, on microstructural properties, monitoring this parameter directly gives information on changes that take place as a result of surface and/or bulk modification processes.

Since the development of a successful reconstruction thermal diffusivity depth profiling algorithm based on the concept of the Hamilton–Jacobi thermal harmonic oscillator,[6,7] several applications in the nondestructive evaluation of hardness depth profiles in steels with various hardening treatments have been reported using photothermal techniques.[8–14] Those studies have found an anticorrelation between thermal diffusivity depth profiles and destructive indenter-induced microhardness measurements. Due to the fact that the thermal-wave amplitude and phase carry information about the heat transport rate through the sample, it is possible to reconstruct the thermal diffusivity depth profile from the experimental data.

The kinetics of light curing resins has been studied extensively in recent years due to its importance in a wide variety of applications including technology and dentistry,[15,16] using various methods based on calorimetry, spectroscopy, mechanics, nuclear and electronic magnetic resonances, etc.[15–18] Those studies have provided useful results toward a better understanding of the complex processes involved.

Recently novel dental resins that can be cured with blue light, exhibiting low shrinkage during the photopolymerization process, have been developed.[19–24] One of the most popular techniques to characterize the degree of polymerization of dental resins is hardness testing. Several authors have found that the tested cured composite resins present gradual decrease in microhardness as depth increases and this decrease is more evident for depths beyond 2 mm.[25–29] This mechanical method provides an important indication of the extent of cure, but it does not directly provide information about the exact amount of light absorbed. Actually, the precise relationship between curing light absorption by the composite material and polymerization depth has not been fully elucidated.

In this paper the thermal diffusivity depth profile of partially cured dental resins is studied using PTR. The samples were coated on one side with a thin layer of gold. Thermal waves were induced on the sample upon illumination of the metallic gold coating with a modulated light source. Photopolymerization was induced by illuminating the opposite side with a nonmodulated blue light. A one-dimensional depth reconstruction model for opaque samples was used to obtain the thermal diffusivity as a function of depth and

[a)]Author to whom correspondence should be addressed. Electronic mail: ptorres@mda.cinvestav.mx.

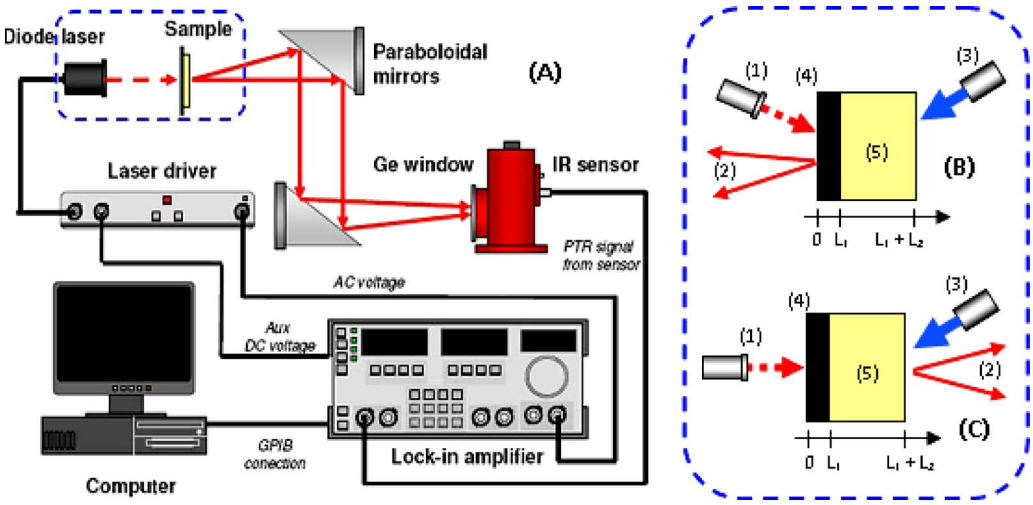

FIG. 1. (Color online) (a) PTR experimental setup, (b) back-propagation configuration, and (c) transmission configuration. (1) Modulated laser diode, (2) emitted modulated IR radiation, (3) continuous curing light, (4) thin metallic film [(b) gold and (c) aluminum], and (5) dental resin.

thickness. It is shown that thermal diffusion is extremely sensitive to the degree of curing of the resin.

II. EXPERIMENTAL SETUP

The experimental PTR system for performing the frequency scans of the samples is shown in Fig. 1. A high power (20 W) laser (Jenoptik JOLD-X-CPXL-1L) was current modulated, at a frequency f, using a ThorLabs high power laser driver. The output diverging beam was collimated, and focused directly onto the surface of the sample with a 5 mm diameter. The laser spot size was expanded in order to generate one-dimensional thermal waves, thereby simplifying the theoretical and computational analyses by avoiding complications due to lateral heat diffusion. This condition was fulfilled when the laser-beam spot size was much larger than the thermal diffusion length at the minimum frequency.[30] The IR radiation from the optically excited sample surface was collected and collimated by two silver-coated, off-axis paraboloidal mirrors and then focused onto a liquid nitrogen cooled HgCdTe (mercury-cadmium-telluride) detector (EG&G Judson J15D12-M204-S01M-60-WE). The heated area of the sample was at the focal point of one mirror and the detector was at the focal point of the other mirror. The detector had an active area of 1 mm^2 and spectral bandwidth of $2-12$ μm. An antireflection coated germanium window with a transmission bandwidth of $2-14$ μm was mounted in front of the detector to block any radiation from the laser. The PTR signal was amplified by a low-noise preamplifier (EG&G Judson PA101) and sent to the digital lock-in amplifier (SR830). The lock-in amplifier received and demodulated the preamplifier output, amplitude, and phase of the PTR signal, which were recorded as functions of frequency in a personal computer. The process of data acquisition, storage, and frequency scanning was fully automated.

In the inset of Fig. 1, the geometry of the investigated sample is represented in its two measurement modalities. It consisted of a resin of thickness L_2, thermal diffusivity α_2, and thermal conductivity k_2, on a metallic film backing of thickness L_1, thermal diffusivity α_1, and thermal conductivity k_1. The two modalities used to perform our experiments were as follows.

(a) *Back-propagation emission configuration.* The modulated laser light illuminated a thin gold metallic film and the IR radiation emitted by the sample was detected on the same film [Fig. 1(b)]. This configuration was used to measure the thermal depth profiles in both intact and partially cured resins. Frequency scans from 4 to 800 Hz were performed on the dental resin composite samples before curing and after partial curing.

(b) *Forward (transmission) emission configuration.* The modulated laser light illuminated an aluminum foil with detection of the periodic radiation on the opposite side [Fig. 1(c)]. This procedure was used to measure the bulk thermal diffusivity of the sample before curing and after curing. The thermal diffusivity of the sample before curing was used as an initial parameter in the algorithm for the reconstruction of the thermal diffusivity depth profile. In this configuration the frequency scan was done from 4 to 23 Hz.

It must be mentioned that one of the principal assumptions is that the sample is opaque to the IR radiation,[24] so that the main contribution to the PTR signal comes from the changes in temperature on the surface of the resin sample. This assumption was found to be true for the thin-film thicknesses used in this work.

III. SAMPLE PREPARATION

The commercial dental resin alert condensable composite (shade A3) manufactured by Pentrol Clinical Technologies, LLC was used in order to obtain a thermal diffusivity depth profile. The introduction of packable resin composites to the market provides an option for the restoration of posterior teeth. They were introduced with the goal of producing handling characteristics similar to amalgam.[19,31]

For the measurements of the thermal diffusivity depth profiles, the resin composite samples were packed into a cyl-

inder of 1 cm diameter and 2 mm height. A glass slide was placed on both faces of the cylinder and gentle pressure was applied to extrude excess material and produce a flat surface. Then, the glass slides were withdrawn and one of the flat surfaces of the sample was gold coated by sputtering deposition until films of around 100 nm thickness were deposited. The purpose of the gold coating was to produce an optically opaque sample in which the metallic film plays the role of a fast light-to-heat converter (around 77 ps).

The gold-coated samples were mounted on the PTR system to obtain the thermal profiles in the back-propagation emission configuration [Fig. 1(b)]. First, a frequency scan in the range from 4 to 800 Hz of the unpolymerized sample was performed. Next, partial polymerization of the dental resin was induced by curing with 30 $\mathrm{mW/cm^2}$ light over 3 min on the opposite surface of the gold coating using a high power blue LED (457 nm). This light was partially absorbed across the resin, generating gradual polymerization of the sample. Following curing, a new frequency scan in the same frequency range was performed for the partially polymerized sample.

In order to measure the bulk thermal diffusivity, flat samples, 400 μm thick, were used before and after the curing process using the forward emission configuration [Fig. 1(c)]. These samples were deposited on top of a 17 μm thick aluminum foil and positioned in the PTR system to be measured in the frequency range from 4 to 23 Hz. In this frequency range the aluminum foil is thermally thin and its purpose is to serve as a rapid light-to-heat converter (around 3 μs) to generate thermal waves in the resin sample.

IV. MATHEMATICAL MODEL OF THE INVERSE PROBLEM

A. Depth profilometric inversion algorithm

The thermal diffusivity depth profiles of the partially cured dental resin samples were determined using the data obtained with the frequency scans, in the back-propagation emission configuration by means of an inversion algorithm. The formalism for the inverse problem methodology of depth profiling of inhomogeneous solids with arbitrary continuously varying thermal diffusivity profiles was developed by Mandelis *et al.*[6] This approach has provided useful results in reconstructing thermal diffusivity profiles from experimental data in various kinds of hardened metals.[8–14]

Considering that the curing light enters the sample on the opposite surface from the gold coating, and that the light is gradually absorbed by the resin along the depth coordinate, thereby producing an inhomogeneous system, the result is also a gradual change in the thermal diffusivity. In view of the fact that the gold film is very thin (100 nm) compared with the sample thickness (2 mm) and taking into account the large laser-beam spot size (5 mm) and that the resin samples were thermally thick in the range of our modulation frequencies, an inversion methodology was used for a one-dimensional semi-infinite solid. The theory assumes that curing affects the thermal diffusivity in a simple functional dependence of the form

$$\alpha_s(x) = \alpha_0 \left(\frac{1 - \Delta e^{-qx}}{1 - \Delta} \right)^2, \tag{1}$$

where

$$\Delta \equiv 1 - \left(\frac{\alpha_0}{\alpha_\infty} \right)^{1/2}, \tag{2}$$

such that $\alpha_s(\infty) = \alpha_\infty$ and $\alpha_s(0) = \alpha_0$; q is a constant that determines the rate of thermal diffusivity growth, with $\alpha_0 < \alpha_\infty$. Although the profile Eq. (1) appears to be a rigid *ad hoc* assumption, in fact, it is very flexible because its parameters can vary with frequency, thus adapting the profile to any local value of diffusivity consistent with the experimental data (photothermal amplitude and phase) at that frequency.

Using the superposition principle in solving the thermal-wave boundary-value problem and forcing the resultant expression to comply with physically expected limiting cases, the expression for the surface thermal wave of a semi-infinite inhomogeneous medium has been shown to be[6]

$$T(0,\omega) = \frac{Q_0}{2\sigma_0 k_0} \left[1 - \frac{1}{4} R_\infty^{1/2} \exp(-\sigma_\infty J_\infty) \right], \tag{3}$$

where

$$J_\infty = \frac{1}{2q} \ln\left(\frac{\alpha_\infty}{\alpha_0} \right), \quad R_\infty = \frac{k_0 \sigma_0}{k_\infty \sigma_\infty}, \tag{4}$$

k_0 is the thermal conductivity of the surface layer, Q_0 is the incident heat flux, and σ_∞ is the complex wave number at distant (bulk) locations in the sample, defined as

$$\sigma_\infty = (1+i)\sqrt{\frac{\omega}{2\alpha_\infty}}. \tag{5}$$

$\omega = 2\pi f$ represents the angular modulation frequency. The theoretical values of amplitude and phase are calculated from

$$T(0,\omega) = |A(\omega)| e^{i\Delta\phi(\omega)}, \tag{6}$$

where $A(\omega)$ is the thermal-wave amplitude and $\Delta\phi(\omega)$ is the phase at angular frequency ω. At each modulation frequency the PTR amplitude and phase are used to calculate α_∞ and q using Eqs. (3)–(6), where α_0 represents the known bulk thermal diffusivity before curing. The actual profile is updated at each frequency by recalculating new parameters of α_∞ and q. Arbitrary depth profiles may be reconstructed by numerically determining the optimal pair of α_∞ and q so that the assumed profile locally results in the experimentally observed thermal-wave signal amplitude and phase data. Therefore, at each ω_j, a system of two equations and two unknown parameters is solved. The calculation for reconstructing the depth parameter x_j is performed based on the fact that, as the modulation frequency decreases, the thermal-wave probing depth increases. Starting at the highest angular frequency ω_0, the shortest depth is the shortest thermal diffusion length, i.e.,

$$x_0 = \sqrt{\frac{2\alpha_0}{\omega_0}}, \tag{7}$$

And the next lower frequency ω_{j+1} corresponds to an increased thermal-wave depth

$$x_{j+1} = x_j + \sqrt{\frac{2\alpha_{s(j)}}{\omega_{j+1}}} - \sqrt{\frac{2\alpha_{s(j)}}{\omega_j}}, \tag{8}$$

which is then substituted into Eq. (1) to calculate $\alpha_{s(j+1)}$. Once $\alpha_{s(j+1)}$ is calculated the method returns to recursively revise and improve the accuracy of the thermal-wave depth slice as

$$x_{j+1} = x_j + \sqrt{\frac{2\alpha_{s(j+1)}}{\omega_{j+1}}} - \sqrt{\frac{2\alpha_{s(j)}}{\omega_j}}. \tag{9}$$

Therefore, the depth of each virtual slice depends on ω_j and $\alpha_{s(j)}$. The true profile is built up by individual slice profiles, with x_0 being the first slice corresponding to the highest frequency. The detailed description of the inversion method can be found elsewhere.[6,7]

B. Thermal diffusivity of homogeneous resin in the transmission mode

An independent measurement of the bulk thermal diffusivity of the dental resin sample before curing is required for the numerical inversion of the frequency scans. This is so because from Eq. (1) it is assumed that the thermal diffusivity before curing (α_0) is known.

It has been shown that the forward (transmission) emission configuration is convenient for measuring the bulk thermal diffusivity, due to the fact that in this case thermal-wave transmission is monitored,[2,5,32] which depends exponentially on thickness and thermal diffusivity.

The thermal-wave field at the back surface of the resin is given by[33]

$$T(L_1 + L_2) = \frac{2\eta I_0}{(\sigma_1 k_1 + \sigma_2 k_2)} \times \left[\frac{e^{-\sigma_1 L_1} e^{-\sigma_2 L_2}}{1 + R(e^{-2\sigma_2 L_2} - e^{-2\sigma_1 L_1}) - e^{-2\sigma_1 L_1} e^{-2\sigma_2 L_2}} \right], \tag{10}$$

where $R = 1 - e_2/e_1$, $\sigma_n = (1+i)/\mu_n$, and $\mu_n = \sqrt{\alpha_n/\pi f}$ is the thermal diffusion length of aluminum foil ($n=1$) and sample ($n=2$). η is the optical-to-thermal (nonradiative) energy conversion efficiency and I_0 is the incident optical intensity. e_1 (α_1) and e_2 (α_2), are the thermal effusivities (thermal diffusivity) of the aluminum foil and sample, respectively.

When the thickness of the aluminum backing is small (thermally thin, $\mu_1 > 2L_1$), in Eq. (10) the approximation $e^{-2\sigma_1 L_1} \approx 1$ can be used and if the resin layer is thermally thick ($\mu_2 < L_2/2$) the approximation $e^{-2\sigma_2 L_2} \ll 1$ follows.[34] Also it is assumed that $L_1 \ll L_2$.

Assuming the simultaneous validity of both approximations, the thermal-wave amplitude is approximately given by

$$T(L_1 + L_2) \approx T(L_2) = \frac{I_0 \eta}{e_2 \sqrt{2\pi}} \frac{e^{-L_2/\mu_2}}{\sqrt{f}}. \tag{11}$$

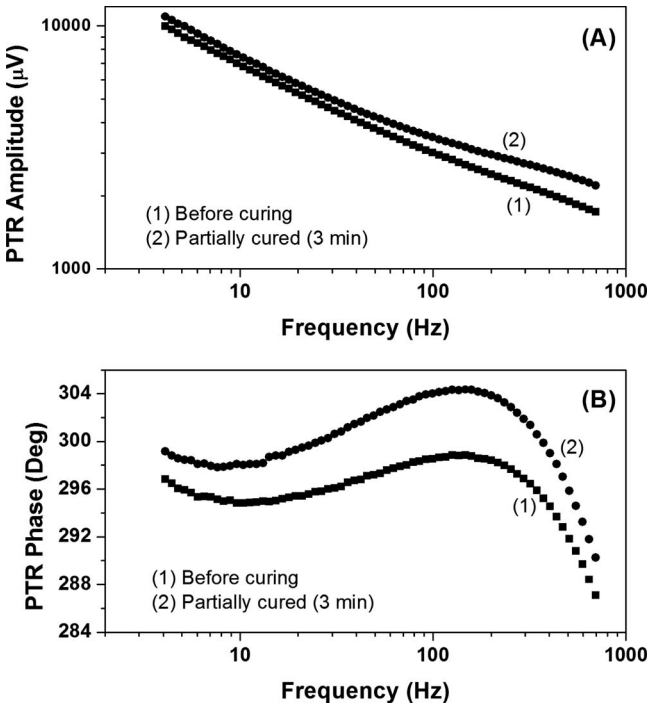

FIG. 2. (a) PTR amplitude and (b) phase signal from the dental resin before and after partial curing.

The amplitude given by Eq. (11) does not only depend on the thermal diffusivity of the sample, but also is inversely proportional to sample thermal effusivity $e_2 = k_2/\alpha_2^{1/2}$.

The phase lag of the thermal-wave field is given by

$$\varphi(L_2) = -\sqrt{\frac{\pi f}{\alpha_2}} L_2 + \varphi_0, \tag{12}$$

where φ_0 is an instrumental constant. By performing a frequency scan, it is possible to determine the thermal diffusivity of the sample with

$$\alpha_2 = \left(\frac{L_2}{m}\right)^2 \pi, \tag{13}$$

where m is the slope of the linear fit of the experimental phase data as a function of the square root of the frequency.

V. RESULTS AND DISCUSSION

Figures 2(a) and 2(b) show the PTR signal amplitude and phase, respectively, for a typical thermally inhomogeneous sample of dental resin before and after partial curing measured in the back-propagated emission configuration. In order to eliminate the detector response, normalization of amplitude and phase of the partially cured sample was performed with respect to the sample before curing. From visual inspection it was assumed that before curing the sample surface was smooth and the dental resin density in the sample holder was uniform. Frequency was scanned from 4 to 800 Hz. The lower limit was dictated by the requirement that heat diffusion in the sample remains one-dimensional (lateral effects are not taken into account) and the upper limit was determined by the fact that surface inhomogeneity effects should not interfere with the bulk measurement.

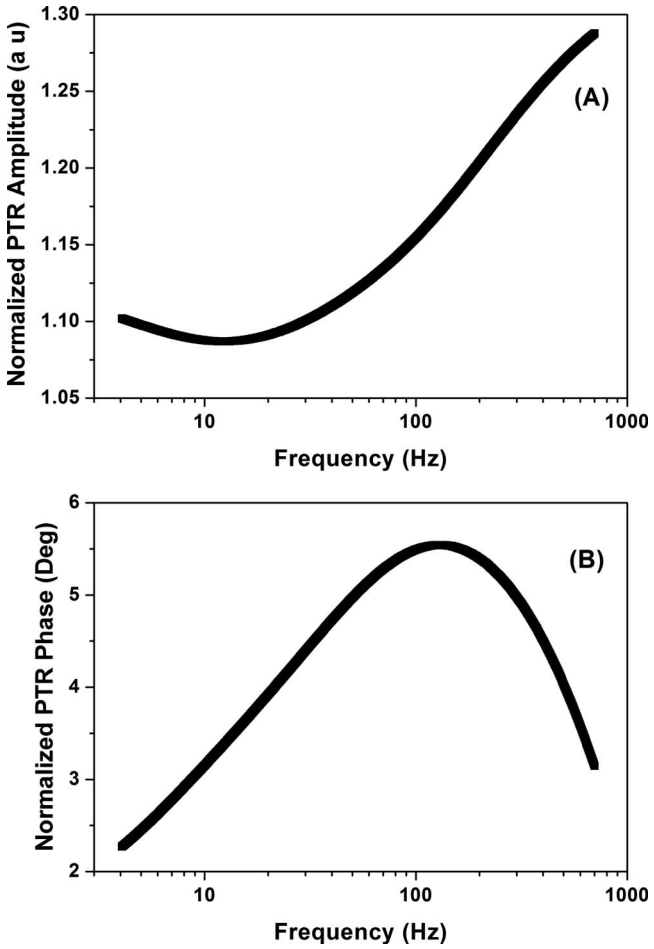

FIG. 3. Normalized PTR signal (a) amplitude ratio and (b) phase difference for a typical partially cured sample. The normalizing reference was the same sample before curing.

Before normalizing, each curve was fitted with a ninth degree polynomial. Using this fit, a set of 700 points was generated in the same frequency range. The polynomial fit was performed to eliminate noise in the signal and reduce the effects of random errors, because the inverse algorithm used to obtain the thermal diffusivity depth profile is very sensitive to the signal-to-noise ratio.[6,7]

Figure 3 shows the PTR signal amplitude and phase of the partially cured sample normalized with respect to the signal before curing. Variations in this amplitude ratio and phase difference with frequency are related to the change in the thermal diffusivity with depth due to the inhomogeneous degree of polymerization in the sample. Note that the optical depth inhomogeneity is not relevant as the surface on which the laser beam impinged was covered with a fully opaque, yet thermally thin, metallic gold coating.

In order to obtain the bulk thermal diffusivity before and after the curing process, the forward configuration presented in Fig. 1(c) was used. As mentioned in Sec. II, in this modality the samples were attached to an aluminum foil (17 μm) to obtain an optically opaque system. Typical experimental phase results from the analyzed resin samples are shown in Fig. 4. This frequency range represents the bulk diffusivity of the sample, which is assumed homogeneous. Fitting the experimental data, for the forward configuration,

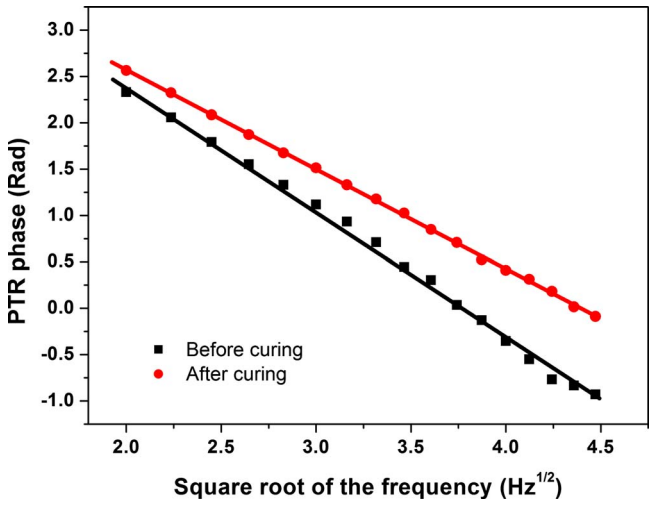

FIG. 4. (Color online) PTR phase signal as a function of square root of the frequency for a typical sample measured in the transmission configuration.

using Eq. (12) provides the parameter m that is used in Eq. (13) to obtain the bulk thermal diffusivity. Typical values for the thermal diffusivity of a 400 μm sample of alert composite A3 before and after the polymerization process are 0.0027 ± 0.0002 and 0.0045 ± 0.0002 cm^2 s^{-1}, respectively.

Using the bulk thermal diffusivity value of the dental resin before curing (α_0=0.0027 cm^2 s^{-1}) measured in the transmission configuration and with the depth profilometric inversion algorithm described above, it is possible to reconstruct the thermal diffusivity depth profile of the partially cured samples measured by the backward emission configuration (Fig. 5). As can be seen, when the depth varies from 10 to 130 μm, all four thermal profiles exhibit an increase in the thermal diffusivity. This increase is due to polymerization and is observed in the bulk thermal diffusivity measurements from the slopes of Fig. 4. This behavior has been reported previously and can be related to a decrease in the monomer density due to the applied blue light and a consequent increase in the polymeric chains.[33]

In our case the gradual change in thermal diffusivity inside the sample can be associated with the attenuation of

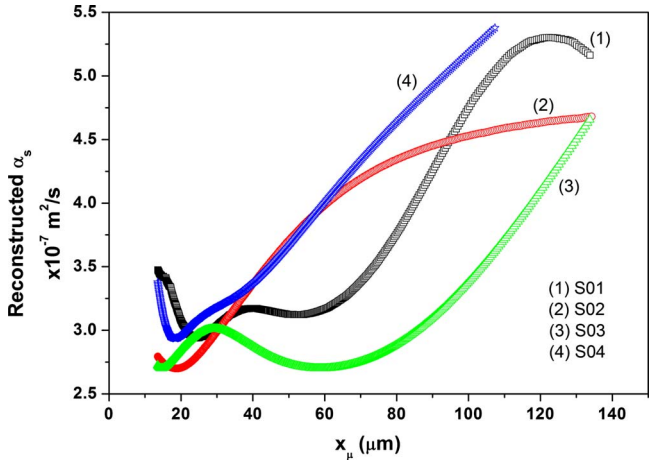

FIG. 5. (Color online) Thermal diffusivity depth profiles for partially cured dental resin samples. x_μ is the reconstructed thermal-wave depth at each modulation frequency.

the curing light intensity entering the sample, generating less photopolymerization in deeper zones of the resin. However, a small increase in thermal diffusivity is invariably observed close to the gold coating. This could be due to the fact that this surface is highly reflective and therefore in this region there exists a higher fluence of blue light compared to the deeper regions. For consistency, it is important to note that far from the coating the reconstruction method using the back-propagation configuration, Fig. 1(b), yields a thermal diffusivity value very close to the bulk thermal diffusivity ($\alpha_\infty = 0.0045\ \mathrm{cm^2\ s^{-1}}$) obtained independently using the transmission configuration [Fig. 1(c)].

It is worth mentioning that the functional dependence of the phase of the PTR signal as a function of the frequency shown in Fig. 4 and obtained in the transmission configuration indicates that in this modality, thermal waves are insensitive to the detailed thermal structure of the sample, only providing a mean value for the bulk thermal diffusivity. In contrast, the back-propagation emission configuration is highly sensitive to the gradual changes generated by the photopolymerization and induces a depth dependent thermal diffusivity.

The results for the thermal diffusivity experimental data can be interpreted in the light of the kinetic equations for the photocuring of polymers,[35] in which the negative time derivative of the monomer concentration is equal to the rate of polymerization R_p that has been shown to be[36]

$$R_p(x,t) = k_p[M(x,t)]\left(\frac{\phi\varepsilon[\mathrm{PI}]I(x)}{k_t}\right)^{1/2}, \tag{14}$$

where k_p is the kinetic rate propagation constant, k_t is the kinetic rate termination constant, $[M]$ is the monomer concentration, ϕ is the quantum yield of the photoinitiator, ε is the molar extinction coefficient, [PI] is the molar concentration of photoinitiator, and $I(x)$ is the absorbed light intensity at depth x, given by Beer's law

$$I(x) = I_0 e^{-\beta x}. \tag{15}$$

Here I_0 is the intensity of light used in the polymerization process absorption and β is the optical absorption coefficient at the blue light wavelength. Substituting Eq. (15) into Eq. (14) and using the kinetic equation for photocuring lead to the following expression:

$$-\frac{\partial[M(x,t)]}{\partial t} = k_p[M(x,t)]\left(\frac{\phi\varepsilon[\mathrm{PI}]I_0}{k_t}\right)^{1/2} e^{-\beta x/2}. \tag{16}$$

Given that the expression in the parentheses on the right-hand side of Eq. (16) is time independent,[36] integration of Eq. (16) yields

$$\ln\left(\frac{[M]_0}{[M(x,t)]}\right) = Ae^{-\beta x/2} \quad \text{with}$$

$$A = \left(\frac{\phi\varepsilon[\mathrm{PI}]I_0}{k_t}\right)^{1/2} k_p t \equiv \frac{t}{\tau}. \tag{17}$$

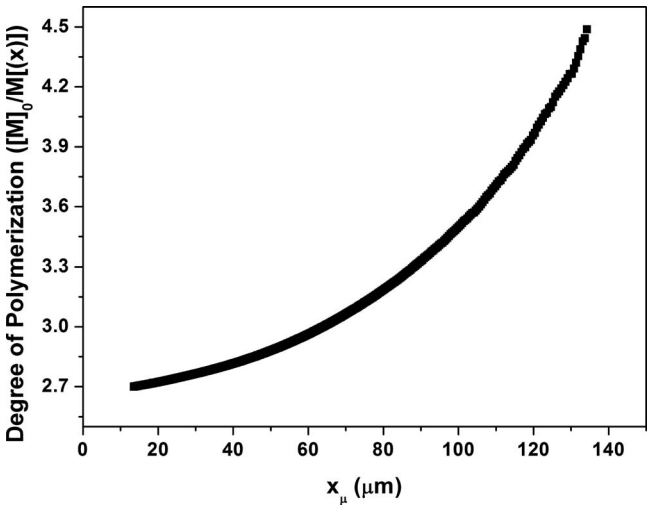

FIG. 6. Degree of polymerization as a function of depth for sample S02 partially cured.

The term in the parentheses on the left-hand side is the degree of polymerization with $[M]_0 \equiv M(x, t=0)$. τ is defined as the polymerization time, i.e., the time required to bring the polymerization process to completion.

For a given exposure time t, and substituting x from Eq. (1) into Eq. (17), a relation between the (mean) degree of polymerization and the depth dependent diffusivity is obtained as follows:

$$\bar{M}(x,t) \equiv \frac{[M]_0}{[M(x)]} = \exp\left[\left(\frac{\sqrt{\alpha_\infty} - \sqrt{\alpha_s(x)}}{\sqrt{\alpha_\infty} - \sqrt{\alpha_0}}\right)^{\beta/2q} \frac{t}{\tau}\right]. \tag{18}$$

This equation provides a simple relationship between the depth dependent thermal diffusivity and the degree of curing through $[M(x,t)]$. Using the reconstructed thermal diffusivity for each depth (Fig. 5) and the associated q values, the degree of polymerization as a function of depth is obtained.

In order to derive numerical results for the degree of polymerization, the typical value $\beta = 1800\ \mathrm{m^{-1}}$ was used for the absorption coefficient of the partially cured resin using blue light (457 nm).[37] Additionally, in view of the fact that the polymerization time (t) used in the experiments is close to the corresponding curing time (τ) with the radiation dose used, the exposure time t may be assumed constant to first approximation, and the factor $A \approx 1$, Eq. (17). Figure 6 shows the degree of polymerization as a function of depth for sample S02. It can be observed that the degree of polymerization decreases from the bulk toward the back surface with respect to the curing light fluence, configuration Fig. 1(b), by ~1.7 times. This trend is expected due to the optical attenuation of the curing blue light source in the resin.

VI. CONCLUSIONS

In this paper we have demonstrated the applicability of PTR as a depth profilometric technique for evaluating the photopolymerization of dental resins, and we have shown its excellent potential as a noncontact, nondestructive quality control methodology for near surface evaluation of the curing process. From PTR measurements of gold coated dental resin samples in the back-propagation emission configuration

it was possible to reconstruct the thermal diffusivity profiles as a function of depth, using a one-dimensional inversion technique.[6] The thermal diffusivity profiles present a smooth increase down to the depth of 120 μm. These results were confirmed by measurements in the transmission configuration that showed a difference of 0.0018 $cm^2\ s^{-1}$ in the bulk thermal diffusivity before and after curing. A relationship between (mean) degree of curing and thermal diffusivity was found. These results indicate that it is possible to analyze the depth dependence of the photopolymerization process using thermal-wave depth profiles.

ACKNOWLEDGMENTS

This work was partially funded by the Multidisciplinary Cinvestav Project 2009 and the CONACyT Becas Mixtas. The support of the Ministry of Research and Innovation (MRI) of Ontario in the form of the 2007 (inaugural) Premier's Discovery Award in Science and Engineering to A.M. is gratefully acknowledged.

[1]H. Vargas and L. C. M. Miranda, Phys. Rep. **161**, 43 (1988).
[2]D. Almond and P. Patel, *Photothermal Science and Techniques* (Chapman and Hall, London, 1996).
[3]A. C. Tam, Rev. Mod. Phys. **58**, 381 (1986).
[4]A. Rosencwaig, *Photoacoustics and Photoacoustic Spectroscopy* (Robert Krieger, Malabar, FL, 1990).
[5]A. Mandelis and P. Hess, *Progress in Photothermal and Photoacoustic Science and Technology: III. Life and Earth Sciences* (SPIE, Bellingham, WA, 1997).
[6]A. Mandelis, J. Math. Phys. **26**, 2676 (1985); A. Mandelis, S. B. Peralta, and J. Thoen, J. Appl. Phys. **70**, 1761 (1991).
[7]A. Mandelis, F. Funak, and M. Munidasa, J. Appl. Phys. **80**, 5570 (1996).
[8]T. C. Ma, M. Munidasa, and A. Mandelis, J. Appl. Phys. **71**, 6029 (1992).
[9]M. Munidasa, Ma. Tian-Chi, A. Mandelis, S. K. Brown, and L. Mannik, Mater. Sci. Eng., A **159**, 111 (1992).
[10]M. Munidasa, F. Funak, and A. Mandelis, J. Appl. Phys. **83**, 3495 (1998).
[11]A. Mandelis, M. Munidasa, and L. Nicolaides, NDT & E Int. **32**, 437 (1999).
[12]L. Nicolaides, A. Mandelis, and C. J. Beingessner, J. Appl. Phys. **89**, 7879 (2001).
[13]Y. Liu, N. Baddour, A. Mandelis, and C. Wang, J. Appl. Phys. **96**, 1929 (2004).
[14]Y. Liu, N. Baddour, A. Mandelis, and C. J. Beingessner, J. Appl. Phys. **96**, 1521 (2004).
[15]A. Andrzejewska, Prog. Polym. Sci. **26**, 605 (2001).
[16]J. P. Fouassier, *Photoinitiation, Photopolymerization, and Photocuring: Fundamentals and Applications* (Hanser Gardner, Cincinnati, OH, 1995).
[17]J. F. Power, Rev. Sci. Instrum. **73**, 4057 (2002).
[18]T. G. Nunes, L. Ceballos, R. Osorio, and M. Toledano, Biomaterials **26**, 1809 (2005).
[19]K. F. Leinfelder, S. C. Bayne, and E. J. Swift, Jr., J. Esthet Dent. **11**, 234 (1999).
[20]K. Kyu-Choi, J. L. Ferracane, T. J. Hilton, and D. Chaklton, J. Esthet Dent. **12**, 216 (2000).
[21]D. S. Cobb, K. M. Macgregor, M. A. Vargas, and G. E. Denehy, J. Am. Dent. Assoc. **131**, 1610 (2000).
[22]J. Manhart, H. Y. Chen, and R. Hickel, J. Am. Dent. Assoc. **132**, 639 (2001).
[23]T. G. Oberholzer, S. R. Grobler, C. H. Pameijer, and R. J. Rossouw, Meas. Sci. Technol. **13**, 78 (2002).
[24]C. Rahiotis, A. Kakaboura, M. Loukidis, and G. Vougiouklakis, Eur. J. Oral Sci. **112**, 89 (2004).
[25]E. P. Allen, S. C. Bayne, A. H. Brodine, R. J. Cronin, Jr., T. E. Donovan, J. C. Kois, and J. B. Summitt, J. Prosthet. Dent. **90**, 50 (2003).
[26]P. C. L. Tsai, I. A. Meyers, and L. J. Walsh, Dent. Mater. **20**, 364 (2004).
[27]J. C. Ciccone-Nogueira, M. C. Borsatto, W. C. Souza-Zaroni, R. Pereira Ramos, and R. G. Palma-Dibb, J. Appl. Oral Sci. **15**, 305 (2007).
[28]K. M. Rode, P. M. de Freitas, P. R. Lloret, L. G. Powell, and M. L. Turbino, Lasers Med. Sci. **24**, 87 (2009).
[29]S. Beun, T. Glorieux, J. Devaux, J. Vreven, and G. Leloup, Dent. Mater. **23**, 51 (2007).
[30]L. Fabbri and F. Cernuschi, J. Appl. Phys. **82**, 5305 (1997).
[31]R. D. Jackson and M. Morgan, J. Am. Dent. Assoc. **131**, 375 (2000).
[32]J. P. Valcárcel M, J. A. Palacios, and J. J. Alvarado-Gil, J. Mater. Sci. **34**, 2113 (1999).
[33]M. A. Zambrano-Arjona, R. Medina-Esquivel, and J. J. Alvarado-Gil, J. Phys. D **40**, 6098 (2007).
[34]A. Rosencwaig and A. Gersho, J. Appl. Phys. **47**, 64 (1976).
[35]G. Odian, *Principles of Polymerization* (Wiley, Hoboken, NJ, 2004).
[36]J. H. Lee, R. K. Prud'homme, and I. A. Aksay, J. Mater. Res. **16**, 3536 (2001).
[37]G. B. dos Santos, R. V. Monte Alto, H. R. Sampaio Filho, E. M. da Silva, and C. E. Fellows, Dent. Mater. **24**, 571 (2008).